WILEY | Hindawi

*Research Article*

# Does Aortic Arch Anatomy Affect Stroke Laterality in Transcatheter Aortic Valve Implantation?

**Caterina Campanella** [ID],[1,2] **Keti Vitanova** [ID],[1,2] **Melchior Burri** [ID],[1,2] **Hendrik Ruge** [ID],[1,2] **Rüdiger Lange** [ID],[1,2,3] **and Stephanie Voss** [ID][1,2]

[1]*Department of Cardiovascular Surgery, German Heart Centre Munich, Technische Universität München, Munich, Germany*
[2]*Insure (Institute of Translational Cardiac Surgery), Department of Cardiovascular Surgery, German Heart Centre Munich, Technische Universität München, Munich, Germany*
[3]*DZHK (German Centre for Cardiovascular Research)-Partner Site Munich Heart Alliance, Munich, Germany*

Correspondence should be addressed to Stephanie Voss; vosss@dhm.mhn.de

*Background*. Current data reveal a predominace of left as opposed to right-sided cerebral strokes after transcatether aortic valve replacement (TAVR). Aortic arch variations might raise the likelihood of cardioembolic particles entering predominantly the left cerebral circulation during catheter tracking and manipulation. *Aim*. We sought to analyse the impact of aortic arch anatomy on stroke laterality (right vs. left) in patients undergoing TAVR. *Methods*. All patients who developed a symptomatic, periprocedural left- or right-sided ischemic stroke after TAVR between June 2007 and August 2022 were included in this study. Multislice computed tomography (MSCT) analysis was used to assess aortic arch anatomy, arch configuration (types I–III), arch tortuosity, and the determination of the take-off angles of the supraaortic arteries. *Results*. The final study cohort comprised 77 patients. Periprocedural ischemic stroke was left-sided in 66.2% of the patients ($n = 51$) and right-sided in 33.8% ($n = 26$) ($p = 0.006$). MSCT analysis revealed a standard aortic arch branching pattern in 70.1% ($n = 54$) and a common origin of the brachiocephalic and left common arteries (bovine arch anatomy) in 29.9% ($n = 23$) of the patients. There was no association between the anatomical variations of the aortic arch and stroke laterality ($p = 0.601$). Frequency of arch configuration types was 15.6% (type I), 74.0% (type II), and 10.4% (type III). There was no correlation between the different types of configuration and the laterality of periprocedural stroke (type I: $p = 0.526$, type II: $p = 0.585$, and type III: $p = 1.000$). Aortic arch tortuosity and angulation of the supraaortic arteries did also not differ between right- and left-sided strokes. *Conclusion*. Our data add evidence that there is a significant propensity for left-hemispheric strokes in patients undergoing TAVR. However, MSCT analysis in our cohort did not reveal an association between aortic arch geometry and laterality of stroke.

## 1. Introduction

Cerebral embolization during transcatheter aortic valve replacement (TAVR) is frequent and causes stroke in up to 2.3%–9.1% of patients [1–5]. Current data from an all-comers analysis investigating 1919 TAVR patients over a 10-year decade revealed a 30-day stroke incidence of 3.4%. In this study, neuroimaging reports detected more often left-sided cardioembolic strokes (45.6%) than right-sided (25%) and bilateral (13.2%) infarctions [6]. In general, left-

hemispheric ischemic strokes have been reported to be associated with a worse clinical outcome than right-hemispheric strokes [7, 8].

Theories behind the predilection for cerebral embolization of the left-brain hemisphere attribute an important role to the anatomical and rheological characteristics of the aortic arch [9–12]. Volumetric flow studies showed that cardioembolic particles have the tendency to slide along the outer curvature of the ascending aorta and to enter the first ostium of the aortic arch branches [10, 13]. Geometrical

variations such as a common origin of the brachiocephalic and left common arteries (bovine arch anatomy) or a sharp angulation of the aortic arch might raise the likelihood of embolic particles entering the left cerebral circulation [10, 11, 13, 14]. Catheter tracking and manipulation during the TAVR procedure might additionally increase the risk of left-sided strokes caused by embolization of mobilized debris in such anatomical constellations [15–17]. Studies investigating the impact of aortic arch variations on stroke localization in TAVR are lacking. We therefore sought to investigate the impact of the aortic arch anatomy on the incidence of stroke laterality during transcatheter aortic valve implantation by multislice computed tomography (MSCT) analysis.

## 2. Materials and Methods

*2.1. Patients.* We conducted a retrospective, MSCT-based analysis of all consecutive patients who developed a symptomatic, right- or left-sided periprocedural ischemic stroke after TAVR at the Department of Cardiovascular Surgery at the German Heart Centre Munich between June 2007 and August 2022. The inclusion criteria for this study were the availability of brain imaging, pre-TAVR aortograms, and manifestation of stroke within 30 days after the procedure. The exclusion criteria were the presence of incomplete or poor-quality MSCT data sets of the aortic arch and its supraaortic branches, aortic dissection, usage of cerebral embolic protection devices, participation in the ongoing prospective randomized PROTECT TAVI trial (clinical-trials.gov NCT02895737 328), significant carotid artery stenosis (>70%) ipsilateral to the stroke, conversion to surgical aortic valve replacement, intraoperative resuscitation, and bilateral and hemorrhagic stroke (Figure 1).

This study complied with the Declaration of Helsinki and was approved by the Local Ethics Committee of the Technical University of Munich (approval reference number: 725/21 SKK).

*2.2. Stroke Classification.* All strokes included fulfilled the Neuro ARC Type I criteria (Valve Academic Research Consortium III) for ischemic, symptomatic stroke according to the latest updated Valve Academic Research Consortium (VARC-III) endpoint definitions [18]. Symptomatic, ischemic stroke was defined as an acute onset of focal neurological signs or symptoms with neuroimaging evidence of CNS infarction in the corresponding brain territory [18].

Neuroimaging reports (brain CT and brain magnetic resonance imaging) were reviewed for classification of stroke laterality. Multiple periprocedural infarcts in the same hemisphere were considered 1 event according to Matakas et al. [13].

According to neuroimaging data, patients were divided into two groups:

(i) Left hemisphere ischemic stroke

New cerebral lesions found in an area supplied by the left common carotid artery and the left posterior inferior cerebellar artery

(ii) Right hemisphere ischemic stroke

New cerebral lesions found in an area supplied by the right innominate artery and the right posterior inferior cerebellar artery

Periprocedural stroke was further subclassified as acute stroke onset, occurring within 24 hours of the index procedure, or as subacute, developing between 24 hours and 30 days [18].

*2.3. MSCT Measurements of the Aortic Arch.* All MSCT measurements were performed with an automated software for 3-dimensional CT reconstruction (3mensio Structural Heart version 10.2, Pie Medical Imaging, Maastricht, the Netherlands) as described previously by the authors [5, 19]. The following parameters were assessed.

*2.3.1. Aortic Arch Anatomy.* Aortic arch anatomy was defined as follows:

(i) *Normal aortic arch* is the separated origin of the brachiocephalic, left common carotid, and left subclavian arteries

(ii) *Bovine arch type I* is the common origin of the brachiocephalic and left common carotid artery

(iii) *Bovine arch type II* is the common origin of the brachiocephalic and left common carotid artery, with the left common carotid artery bifurcating at an average distance of ≤1 cm from the origin [13].

*2.3.2. Aortic Arch Configuration.* Arch configuration according to the outer and inner curvature of the aortic arch was assessed as described previously by the authors [5, 20] and categorized as follows [5]:

(i) *Aortic arch type I*: all supraaortic branches originate from the aortic arch at the level of the first line (Figure 2(a))

(ii) *Aortic arch type II*: at least one of the supraaortic branches originates between the two lines (Figure 2(b))

(iii) *Aortic arch type III*: at least one of the supraaortic branches originates at the level or below the second line (Figure 2(c)).

*2.3.3. Aortic Arch Curvature.* Aortic arch curvature was assessed by determining the maximal aortic arch angulation (AAA) and the aortic arch tortuosity index (TI). 3-mensio imaging analysis initially included automatic extraction of a three-dimensional (3D) center line along the vascular course of the aortic arch, which was manually adjusted to obtain the most accurate measurement.

For evaluation of AAA, two reference points were selected along the center line at the level of the bifurcation of the pulmonary trunk and at the level of the fourth thoracic vertebra body upper edge according to Boufi et al. [21]
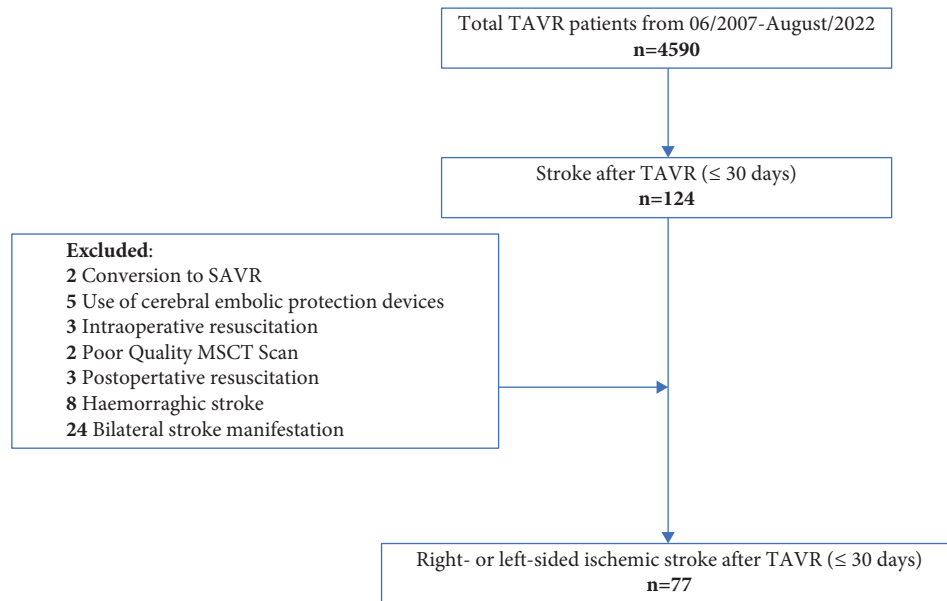
FIGURE 1: Flow diagram of the study population.
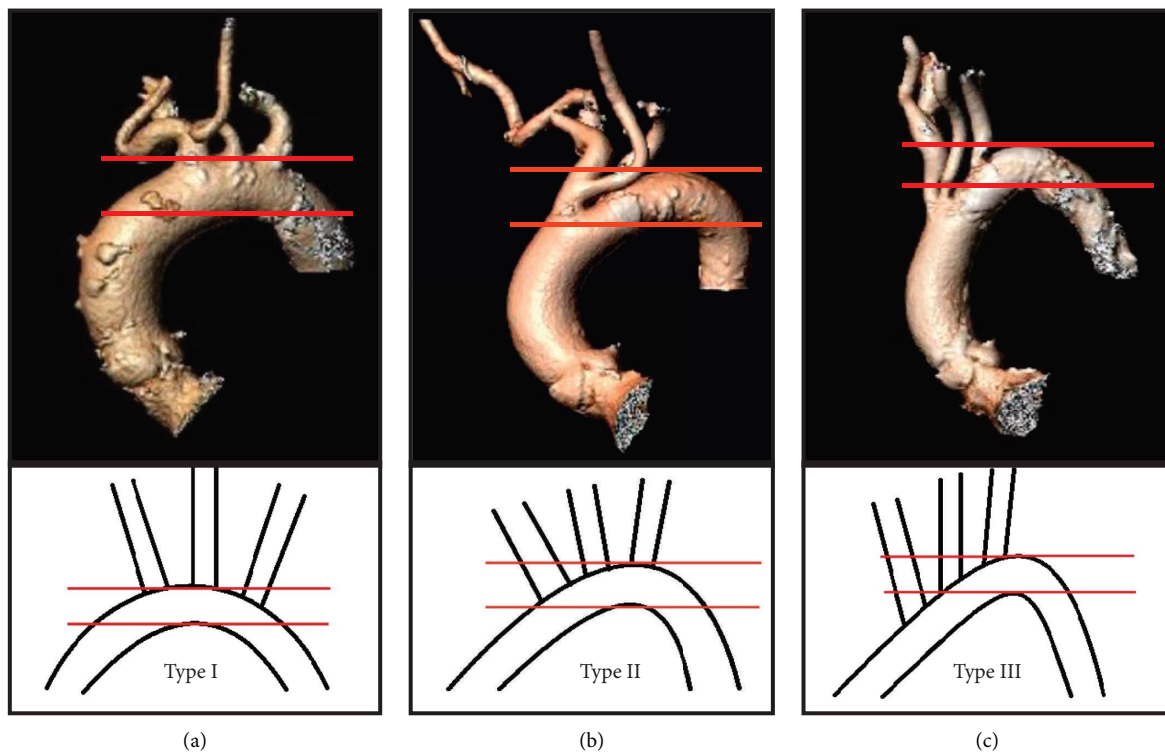


FIGURE 2: Aortic arch configuration according to the origin of the supraaortic arteries, demonstrating a type I (a), type II (b), and type III (c) aortic arch.

(Figure 3). Then, two planes were generated perpendicular to the center line at the marked points. The maximal measured angle between these two planes was defined as the aortic arch angulation (Figure 4).

The TI of the aortic arch was determined by calculating an aortic arch distance factor: [(center-line distance)/ (straight-line distance) − 1] × 100 [5, 21]. The center-line distance reflects the incremental true length of the aorta along the previously defined 3D center line between the marked reference points, while the straight-line distance indicates the linear distance between the landmarks (Figure 5).

(a)



(b)

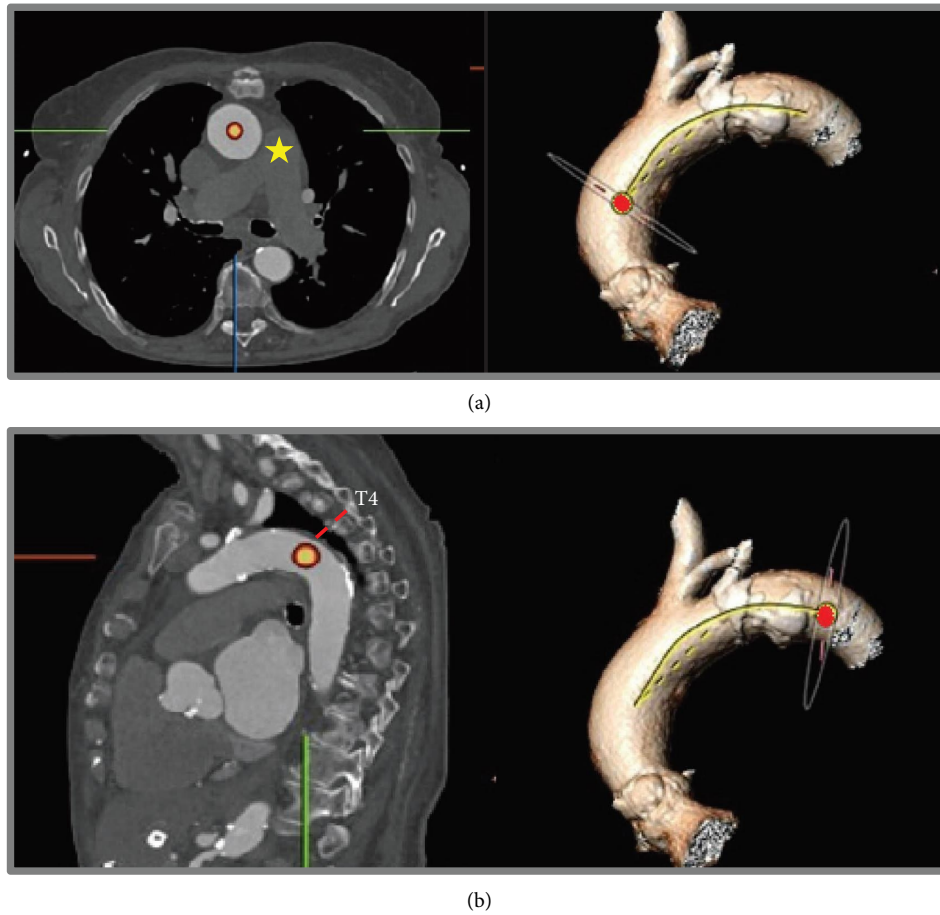FIGURE 3: 3-dimensional center line along the vascular course of the aortic arch between the marked reference points for determination of aortic arch curvature. (a) Proximal landmark at the level of the bifurcation of the pulmonary trunk (*); (b) distal landmark at the level of the fourth thoracic vertebra body upper edge.



(a)         (b)         (c)
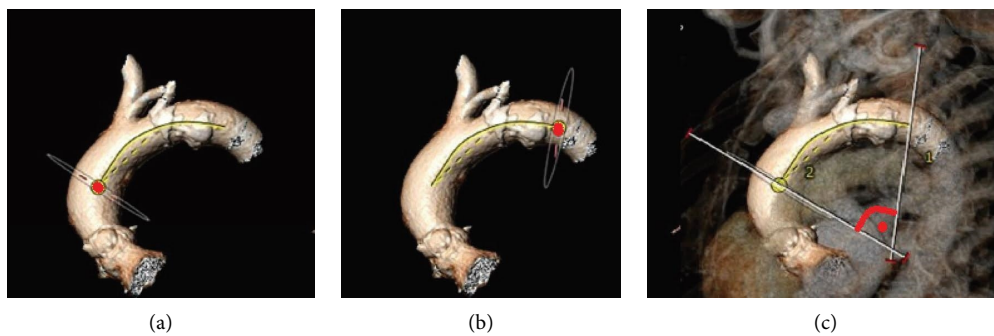
FIGURE 4: Determination of aortic arch angulation.

### 2.3.4. Take-Off Angles of the Supraaortic Arteries.

Measurement of the take-off angles of the supraaortic arteries included the determination of the following angles as described previously [5]:

  (i) Angle between the aorta and the brachiocephalic artery (AA/BA angle)

  (ii) Angle between the aorta and the left common carotid artery (AA/LCC angle)

Interobserver and intraobserver reliability for all computer tomographic measurements was assessed as described previously in detail by the authors [5, 22]. The measurements were performed by two independent cardiac surgeons with long-standing expertise in cardiovascular imaging.

### 2.4. Clinical Data Analysis.

Demographics, procedural details, and postoperative data were recorded according to the latest VARC-3 recommendations in our dedicated TAVR database [18]. Baseline data analyses included patient age, gender, weight, Society of Thoracic Surgeons (STS) Predicted Risk of Mortality Score, EuroSCORE II, chronic kidney disease, history of stroke, peripheral arterial disease,

FIGURE 5: Calculation of the aortic arch tortuosity index.
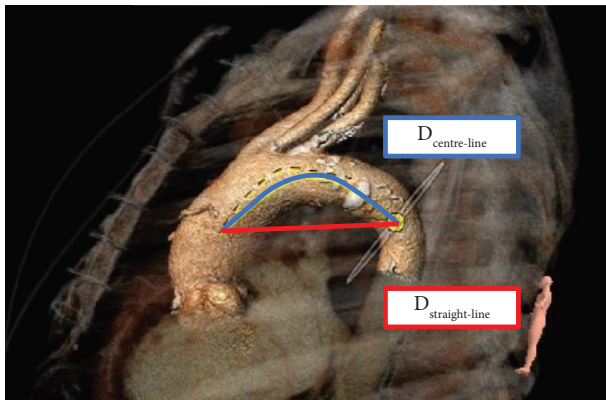
atrial fibrillation (AF), diabetes mellitus type II, dyslipidemia, arterial hypertension, and coronary artery disease. Periprocedural factors were vascular access sites, types of transcatheter heart valve (THV), pre-balloon and post-balloon dilatation, and intraoperative valve embolization.

*2.5. Statistical Analysis.* Statistical analysis was assessed by using IBM SPSS Statistics 22.0 software (IBM Corp, Armonk, NY USA). Frequencies are given as absolute numbers and percentages, continuous data as the median and range. Continuous variables were analyzed using either the two-sided *t*-test or the Mann–Whitney U test [5]. Categorical variables were compared using Fisher's exact test. ICC estimates and their 95% confident intervals (CIs) were calculated based on the two-way random effects, absolute agreement, and multiple raters/measurements ICC model (2, *k*) as described previously [5, 22]. ICC values were classified as follows: values < 0.5 had poor reliability, values between 0.5 and 0.75 had moderate reliability, values between 0.75 and 0.9 had good reliability, and values > 0.90 had excellent reliability. A *p* value less than 0.05 was considered statistically significant.

## 3. Results

A total of 4,590 patients underwent TAVR between June 2007 and August 2022 in our department. Among these, 124 patients developed a periprocedural stroke. Forty-seven patients were excluded from the analysis either due to conversion to surgical aortic valve replacement ($n = 2$), the use of cerebral embolic protection devices ($n = 5$), intraoperative and early postoperative resuscitation ($n = 6$), poor-quality MSCT scans ($n = 2$), hemorrhagic stroke ($n = 8$), and bilateral stroke manifestation ($n = 24$). Therefore, the study cohort comprised 77 patients of whom 66.2% ($n = 51$) suffered a left-sided stroke and 33.8% ($n = 26$) a right-sided stroke ($p = 0.006$). The mean age at the time of TAVR was $79.8 \pm 7.6$ years, and the median EuroSCORE II and STS Score were 3.4 [1.1–22] and 3.0 [1.2–19.5], respectively. Further baseline characteristics are displayed in Table 1, showing no difference between the study groups (right-vs. left-sided stroke).

In total, 46 self-expandable (SEV) and 31 balloon-expandable (BEV) transcatheter heart valves were implanted via transfemoral ($n = 65$), transaortal ($n = 4$), transapical ($n = 7$), and transaxillary ($n = 1$) access. TAVR valve type, access route, and balloon predilatation and postdilatation did not differ between TAVR patients with right-sided and left-sided stroke manifestation (Table 2). In 41.6% of the patients ($n = 32/77$), post-TAVR stroke occurred within 24 h after the index procedure, whereas 58.4% suffered from a subacute periprocedural stroke.

MSCT measurements revealed no significant difference regarding the anatomy and configuration of the aortic arch in TAVR patients with right-sided and left-sided ischemic strokes (Table 3). Normal aortic arch anatomy and type II arch configuration were the most frequently observed morphologies in patients with right- and left-sided strokes, with 65.4% and 72.5% and 69.2% and 76.5%, respectively. Determination of the supraaortic take-off angles did not show any difference between right- and left-sided brain infarctions (AA/BA angle: $p = 0.620$; AA/CCA: $p = 0.337$). Calculation of aortic arch angulation (right-sided 95.5° [63–141] vs. left-sided 88.0° [27–132]; $p = 0.267$) and aortic arch TI (right-sided 15.8 [8.3-45.7] vs. left-sided 14.6 [0.4–41.5]; $p = 0.0526$) was also similar in both groups (Table 3).

Assessment of interobserver and intraobserver reproducibility revealed an overall mean ICC of 0.982 (inter-) and 0.970 (intra-). The detailed results of the calculation for each MSCT parameter are included in Supplementary Materials (Supplement Tables 1 and 2).

## 4. Discussion

Since 2002 TAVR has emerged as an established treatment option in patients with aortic stenosis [23, 24]. However, TAVR-associated embolic strokes remain one of the most feared complications, significantly affecting survival and quality of life [25, 26]. Recent data from an all-comers analysis ($n = 1919$) suggest a hemispheric predilection for stroke associated with TAVR [6]. While it seems intuitively conceivable that anatomical variations like a severely angulated arch or a complex bovine arch configuration might affect the direction of embolic material, there are no clinical studies that objectively characterize this hypothesis in TAVR patients.

Prior computer-based volumetric flow models of the aortic arch suggested a correlation of arch morphology and corresponding stroke laterality [10, 27, 28]. However, this could not be confirmed clinically in our study. Based on a 3-dimensional MSCT analysis, aortic arch anatomy in our patients had no influence on hemispheric distribution of post-TAVR stroke. In line with previous studies [6, 11], a higher propensity of left-sided ischemic infarctions could be detected in our patients. We initially hypothesized that bovine arch configuration might be an important determinant for embolic stroke localization [13, 14]. Previous biomechanical flow studies indicated that embolic particles have the tendency to slide along the outer curvature of the ascending aorta entering the first ostium of the aortic arch

TABLE 1: Baseline data.

| Characteristics | Right-sided stroke $n = 26$ | Left-sided stroke $n = 51$ | $p$ value |
|---|---|---|---|
| Age, years (median, range) | 80.4 (64.0–94.0) | 79.4 (52.0–90.0) | 0.586 |
| Female, $n$ (%) | 18 (69.2) | 29 (56.9) | 0.332 |
| Body mass index, kg/m$^2$ (median, range) | 27.1 (19.7–46.8) | 26.5 (19.6–53.8) | 0.779 |
| Diabetes mellitus type II, $n$ (%) | 6 (23.1) | 15 (29.4) | 0.601 |
| Dyslipidemia, $n$ (%) | 22 (84.6) | 38 (74.5) | 0.392 |
| Arterial hypertension, $n$ (%) | 24 (92.3) | 49 (96.1) | 0.600 |
| Atrial fibrillation, $n$ (%) | 7 (26.9) | 17 (33.3) | 1.000 |
| History of stroke, $n$ (%) | 5 (19.2) | 8 (15.7) | 0.752 |
| Peripheral arterial disease, $n$ (%) | 3 (11.5) | 12 (23.5) | 0.243 |
| Chronic kidney disease, $n$ (%) | 6 (23.1) | 17 (33.3) | 0.435 |
| Coronary artery disease, $n$ (%) | 15 (57.7) | 34 (66.7) | 0.463 |
| Left ventricular ejection fraction ≤50%, $n$ (%) | 7 (26.9) | 14 (27.5) | 1.000 |
| EuroSCORE II (median, range) | 3.1 (1.1–22.0) | 3.6 (1.2–19.6) | 0.294 |
| Society of thoracic surgeons score (median, range) | 3.1 (1.2–19.5) | 2.9 (1.2–17.1) | 0.718 |

TABLE 2: Periprocedural data.

| Patient characteristics | Right-sided stroke $n = 26$ | Left-sided stroke $n = 51$ | $p$ value |
|---|---|---|---|
| *Intraoperative characteristics* | | | |
| Predilatation, $n$ (%) | 14 (53.8) | 29 (56.9) | 0.831 |
| Postdilatation, $n$ (%) | 5 (19.2) | 15 (29.4) | 0.417 |
| Self-expandable valve, $n$ (%)* | 19 (73.1) | 27 (52.9) | 0.140 |
| Balloon-expandable valve, $n$ (%)# | 7 (26.9) | 24 (47.1) | 0.140 |
| Valve embolization, $n$ (%) | 1 (3.8) | 5 (9.8) | 0.657 |
| *Access route, $n$ (%)* | | | |
| (i) Transfemoral | 23 (88.5) | 42 (82.4) | 0.741 |
| (ii) Transaortal | 1 (3.8) | 3 (5.9) | 1.000 |
| (iii) Transapical | 2 (7.7) | 5 (9.8) | 1.000 |
| (iv) Subclavian | 0 (0.0) | 1 (2.0) | 1.000 |

*Transcatheter heart valves used: $n = 21$ Medtronic CoreValve, $n = 9$ Medtronic Evolut R, $n = 5$ Medtronic Evolut PRO, $n = 4$ JenaValve, $n = 4$ Boston Scientific LOTUS, and $n = 2$ Symetis ACURATE neo; #transcatheter heart valves used: $n = 5$ Edwards Sapien XT, $n = 13$ Edwards Sapien 3, and $n = 14$ Edwards Sapien ultra.

TABLE 3: MSCT measurements.

| Patient characteristics | Right-sided stroke $n = 26$ | Left-sided stroke $n = 51$ | $p$ value |
|---|---|---|---|
| *Aortic arch anatomy, n, (%)* | | | |
| (i) Normal | 17 (65.4%) | 37 (72.5%) | 0.601 |
| (ii) Bovine type I | 7 (26.9%) | 13 (25.5%) | 1.000 |
| (iii) Bovine type II | 2 (7.7%) | 1 (2.0%) | 0.262 |
| *Aortic arch configuration, n, (%)* | | | |
| (i) Type I | 5 (19.2%) | 7 (13.7%) | 0.526 |
| (ii) Type II | 18 (69.2%) | 39 (76.5%) | 0.585 |
| (ii) Type III | 3 (11.5%) | 5 (9.8%) | 1.000 |
| *Take-off angle, degree (median, range)* | | | |
| (i) AA/BA | 109.0 (70.0–145.0) | 113.0 (58.0–137.0) | 0.620 |
| (ii) AA/CCA | 129.5 (94.0–165.0) | 126.0 (95.0–162.0) | 0.337 |
| Aortic arch angulation, degree (median, range)* | 95.5 (63.0–141.0) | 88.0 (27.0–132.0) | 0.267 |
| Aortic arch tortuosity index (median, range)* | 15.8 (8.3–45.7) | 14.6 (0.4–41.5) | 0.527 |

*Aortic arch angulation and aortic arch tortuosity index measurement were only performed in 69 and 70 patients, respectively, due to insufficient 3-dimensional MSCT reconstructions.

branches [8, 10]. In the standard aortic arch, the brachiocephalic artery represents the first branch, which runs upwards and parallel to the direction of the ascending aorta, raising the likelihood of embolic particles entering the right cerebral circulation [13, 14]. In case of the bovine arch, the brachiocephalic trunk and the left common carotid artery share the same origin resulting in a more oblique vessel orientation of the left common carotid artery. This, in turn, might be more aligned with the trajectories of arriving embolic material [11, 13]. Despite a bovine arch prevalence

of 29.9% (23/77) in our study cohort, which is higher than the general population-based incidence of 8–25% [7, 9, 29], no difference in stroke laterality could be observed. Similar to our findings, Gold et al. also showed no significant difference in right-left propensity of cerebral infarcts comparing standard with the bovine arch in 119 patients suffering from cardioembolic, non-TAVR related stroke [14].

In contrary, a recently published study by Mataka and colleagues supported a correlation of aortic arch anatomy and hemispheric laterality in a large investigation of 615 patients with acute cardioembolic brain infarcts due to atrial fibrillation [13]. MSCT measurements in this study revealed a significant propensity for left-sided cerebral cardioembolic infarcts in patients with bovine configuration [13]. One reason for the inconsistent study findings might be the difference in the analyzed cohorts. While the study population by Mataka et al. focused on patients suffering from spontaneous, non-perioperative strokes, our study cohort compromised procedure-related cerebral infarctions. Embolic clot motion in our patients might be different. Acute stroke following TAVR predominantly is due to embolization arising from particulate matter during advancement of THV devices and THV deployment [30]. Intravascular devise manipulations might induce flow disturbances potentially affecting clot trajectory and right-left stroke propensity.

Among the branching pattern of the aortic arch, arch steepness is also thought to be associated with stroke laterality [11, 27, 28]. Choi et al. performed fluid dynamic simulations using patient-dependent aorta models suggesting that aortic steepness might be an important risk factor for propensity of stroke distribution [28]. In case of a steep arch morphology, the left common carotid artery runs parallel to the inlet flow stream which might result in more emboli entering this side [27]. Arch steepness in our TAVR analysis was represented by evaluation of aortic arch configuration (types I–III) and arch angulation. We found a type II steep aortic arch to be the most common configuration in our patients (74.0%), with a median arch angulation of 90°degree. However, arch steepness in our clinical analysis was no predictor for stroke laterality in TAVR-associated strokes. Thus, the assumptions made in the biomechanical studies could not be confirmed in our clinical study setting. Also, Elsaid and colleagues found no significant correlation between arch angulation and left-sided stroke propensity in 192 patients with cardioembolic cerebral infarction [11].

## 5. Limitations

Our study reports the results of a retrospective, single-center investigation of limited size. As the primary outcome was the relationship between stroke laterality and the underlying aortic arch anatomy in TAVR-associated stroke, stroke severity and associated disability were not assessed. In addition, study results might be confounded by procedural factors such as operators' experience, TAVR access routes, and advances in techniques over the study period, as well as postprocedural factors such as atrial fibrillation and initiation of sufficient anticoagulation.

## 6. Conclusion

Our data add evidence that periprocedural stroke after TAVR is associated with left-hemispheric predilection. However, there was no correlation between aortic arch morphology and stroke laterality. Based on the anatomy of the aortic arch, it is therefore not possible to predict the risk of periprocedural TAVR-associated stroke.

## Abbreviations

| | |
|---|---|
| AAA: | Aortic arch angulation |
| AA/BA angle: | Aortic arch/brachiocephalic artery angle |
| AA/LCCA angle: | Aortic arch/left common carotid artery angle |
| AF: | Atrial fibrillation |
| BEV: | Balloon-expandable valve |
| BT: | Brachiocephalic trunk |
| LCCA: | Left common carotid artery |
| ICC: | Intraclass correlation coefficient |
| MSCT: | Multislice computed tomography |
| MRI: | Magnetic resonance imaging |
| SEV: | Self-expandable valve |
| VARC 3: | Valve Academic Research Consortium III |
| TAVR: | Transcatheter aortic valve replacement |
| THV: | Transcatheter heart valve |
| TI: | Tortuosity index. |

## Data Availability

The MSCT data used to support the findings of this study are available from the corresponding author upon request.

## Conflicts of Interest

The authors declare that there are no conflicts of interests.

## Acknowledgments

## Supplementary Materials

Estimated interobserver and intraobserver agreement for each MSCT parameter including their 95% confident intervals is given in Tables 1 and 2. (*Supplementary Materials*)

## References

[1] C. P. Huded, E. M. Tuzcu, A. Krishnaswamy et al., "Association between transcatheter aortic valve replacement and early postprocedural stroke," *JAMA*, vol. 321, no. 23, pp. 2306–2315, 2019.

[2] S. R. Kapadia, S. Kodali, R. Makkar et al., "Protection against cerebral embolism during transcatheter aortic valve

replacement," *Journal of the American College of Cardiology*, vol. 69, no. 4, pp. 367–377, 2017.

[3] F. Muscente and R. De Caterina, "Risk of stroke after transcatheter aortic valve implant: the role of the new oral anticoagulants," *European Heart Journal Supplements*, vol. 21, no. Supplement_B, pp. B50–B51, 2019.

[4] A. Muralidharan, K. Thiagarajan, R. Van Ham et al., "Meta-analysis of perioperative stroke and mortality in transcatheter aortic valve implantation," *The American Journal of Cardiology*, vol. 118, no. 7, pp. 1031–1045, 2016.

[5] S. Voss, C. Campanella, M. Burri et al., "Anatomical reasons for failure of dual-filter cerebral embolic protection application in TAVR: a CT-based analysis," *Journal of Cardiac Surgery*, vol. 36, no. 12, pp. 4537–4545, 2021.

[6] L. K. Eschenbach, M. Erlebach, M. A. Deutsch, H. Ruge, S. Bleiziffer, and L. Holzer, "Stroke after transcatheter aortic valve replacement: a severe complication with low predictability. Catheterization and cardiovascular interventions," *Official Journal of the Society for Cardiac Angiography and Interventions*, vol. 9, no. 6, 2022.

[7] V. S. Hedna, A. N. Bodhit, S. Ansari et al., "Hemispheric differences in ischemic stroke: is left-hemisphere stroke more common?" *Journal of Clinical Neurology*, vol. 9, no. 2, pp. 97–102, 2013.

[8] C. Grefkes and G. R. Fink, "Recovery from stroke: current concepts and future perspectives," *Neurological Research and Practice*, vol. 2, no. 1, p. 17, 2020.

[9] L. Prahl Wittberg, S. van Wyk, L. Fuchs, E. Gutmark, P. Backeljauw, and I. Gutmark-Little, "Effects of aortic irregularities on blood flow," *Biomechanics and Modeling in Mechanobiology*, vol. 15, no. 2, pp. 345–360, 2016.

[10] I. A. Carr, N. Nemoto, R. S. Schwartz, and S. C. Shadden, "Size-dependent predilections of cardiogenic embolic transport," *American Journal of Physiology Heart and Circulatory Physiology*, vol. 305, no. 5, pp. H732–H739, 2013.

[11] N. Elsaid, G. Bigliardi, M. L. Dell'Acqua et al., "The relation between aortic arch branching types and the laterality of cardio-embolic stroke," *Journal of Stroke and Cerebrovascular Diseases*, vol. 29, no. 7, Article ID 104917, 2020.

[12] S. K. Aggarwal, N. Delahunty Rn, L. J. Menezes et al., "Patterns of solid particle embolization during transcatheter aortic valve implantation and correlation with aortic valve calcification," *Journal of Interventional Cardiology*, vol. 31, no. 5, pp. 648–654, 2018.

[13] J. D. Matakas, M. M. Gold, J. Sterman et al., "Bovine arch and stroke laterality," *Journal of the American Heart Association*, vol. 9, no. 13, Article ID e015390, 2020.

[14] M. Gold, M. Khamesi, M. Sivakumar, V. Natarajan, H. Motahari, and N. Caputo, "Right-left propensity of cardiogenic cerebral embolism in standard versus bovine aortic arch variant," *Clinical Anatomy*, vol. 31, no. 3, pp. 310–313, 2018.

[15] J. Bismuth, Z. Garami, J. E. Anaya-Ayala et al., "Transcranial Doppler findings during thoracic endovascular aortic repair," *Journal of Vascular Surgery*, vol. 54, no. 2, pp. 364–369, 2011.

[16] H. Rafii-Tari, C. J. Payne, and G.-Z. Yang, "Current and emerging robot-assisted endovascular catheterization technologies: a review," *Annals of Biomedical Engineering*, vol. 42, no. 4, pp. 697–715, 2014.

[17] H. Rafii-Tari, C. V. Riga, C. J. Payne et al., "Reducing contact forces in the arch and supra-aortic vessels using the Magellan robot," *Journal of Vascular Surgery*, vol. 64, no. 5, pp. 1422–1432, 2016.

[18] P. Généreux, N. Piazza, M. C. Alu et al., "Valve Academic Research Consortium 3: updated endpoint definitions for aortic valve clinical research," *European Heart Journal*, vol. 42, no. 19, pp. 1825–1857, 2021.

[19] S. Voss, J. Schechtl, C. Nobauer, S. Bleiziffer, and R. Lange, "Patient Eligibility for Application of a Two-Filter Cerebral Embolic protection Device during Transcatheter Aortic Valve Implantation: Does One Size Fit All?" *Interactive Cardiovascular and Thoracic Surgery*, vol. 30, no. 4, pp. 605–612, 2020.

[20] M. D. Muller, F. J. Ahlhelm, A. von Hessling, P. Nederkoorn, S. Macdonald, and P. Lyrer, "Vascular anatomy predicts the risk of cerebral ischemia in patients randomized to carotid stenting versus endarterectomy," *Journal of Vascular Surgery*, vol. 66, no. 1, pp. 327–392, 2017.

[21] M. Boufi, C. Guivier-Curien, A. D. Loundou et al., "Morphological analysis of healthy aortic arch," *European Journal of Vascular and Endovascular Surgery*, vol. 53, no. 5, pp. 663–670, 2017.

[22] T. K. Koo and M. Y. Li, "A guideline of selecting and reporting intraclass correlation coefficients for reliability research," *Journal of Chiropractic Medicine*, vol. 15, no. 2, pp. 155–163, 2016.

[23] C. R. Smith, M. B. Leon, M. J. Mack et al., "Transcatheter versus surgical aortic-valve replacement in high-risk patients," *New England Journal of Medicine*, vol. 364, no. 23, pp. 2187–2198, 2011.

[24] J. J. Popma, D. H. Adams, M. J. Reardon et al., "Transcatheter aortic valve replacement using a self-expanding bioprosthesis in patients with severe aortic stenosis at extreme risk for surgery," *Journal of the American College of Cardiology*, vol. 63, no. 19, pp. 1972–1981, 2014.

[25] J. D. Salazar, R. J. Wityk, M. A. Grega et al., "Stroke after cardiac surgery: short- and long-term outcomes," *The Annals of Thoracic Surgery*, vol. 72, no. 4, pp. 1195–1201, 2001.

[26] F. Filsoufi, P. B. Rahmanian, J. G. Castillo, D. Bronster, and D. H. Adams, "Incidence, imaging analysis, and early and late outcomes of stroke after cardiac valve operation," *The American Journal of Cardiology*, vol. 101, no. 10, pp. 1472–1478, 2008.

[27] F. Malone, E. McCarthy, P. Delassus, J. H. Buhk, J. Fiehler, and L. Morris, "Embolus analog trajectory paths under physiological flowrates through patient-specific aortic arch models," *Journal of Biomechanical Engineering*, vol. 141, no. 10, Article ID 101007, 2019.

[28] H. W. Choi, T. Luo, J. A. Navia, and G. S. Kassab, "Role of aortic geometry on stroke propensity based on simulations of patient-specific models," *Scientific Reports*, vol. 7, no. 1, p. 7065, 2017.

[29] A. P. Tagliari, E. Ferrari, P. K. Haager et al., "Feasibility and safety of cerebral embolic protection device insertion in bovine aortic arch anatomy," *Journal of Clinical Medicine*, vol. 9, no. 12, p. 4118, 2020.

[30] J. K. Devgun, S. Gul, D. Mohananey et al., "Cerebrovascular events after cardiovascular procedures: risk factors, recognition, and prevention strategies," *Journal of the American College of Cardiology*, vol. 71, no. 17, pp. 1910–1920, 2018.